

# 1 **Coupled Evolution of Topography and Orographic Precipitation in Varied Climates**

2

3 Alison M. Anders<sup>1</sup>, Gerard H. Roe<sup>2</sup>, David R. Montgomery<sup>2</sup>, Bernard Hallet<sup>2</sup>

4

5 <sup>1</sup> University of Washington, Department of Earth and Space Sciences, now at University of Illinois,  
6 Department of Geology

7 <sup>2</sup> University of Washington, Department of Earth and Space Sciences

8

## 9 **Abstract**

10

11 Precipitation patterns in mountain ranges are strongly controlled by topography, highly variable in  
12 space, and persistent over timescales for which measurements exist. The impact of spatial  
13 patterning of precipitation on landscape evolution is examined with a coupled model of orographic  
14 precipitation and surface erosion. For a range of plausible climate variables, steady-state  
15 precipitation patterns vary from nearly uniform and maximizing over the highest topography to  
16 highly spatially variable, closely coupled to small-scale topography and maximizing low on  
17 windward slopes. Such precipitation patterns are a first-order control on significant aspects of  
18 modeled landscape morphology including range scale and ridge-valley scale relief, channel  
19 concavity, and the position of the main drainage divide. An association between more uniform  
20 precipitation patterns and cooler climates is suggested based on field studies and the strong  
21 dependence of precipitation fall speed (and hence advection distance) on precipitation phase. The  
22 coupled evolution of precipitation patterns and topography further demonstrates the fundamental  
23 importance of the coupled climate, erosion and tectonic system for mountain geomorphology.

24

25

26 **Motivation and Model Framework**

27

28 It is axiomatic that precipitation exerts some control on nearly all erosional processes and thereby  
29 influences landscape evolution. Precipitation accumulated as river discharge is fundamental in  
30 driving landscape change and the geodynamic evolution of active orogens (e.g., Whipple, 2004),  
31 and glacial erosion rates likewise scale with ice discharge and thus with the precipitation rate of  
32 snow (e.g. Hallet, 1996). However, precipitation is not simply a driver of erosion and a cause of  
33 topographic change; it is strongly influenced by topography in mountainous regions. Thus the  
34 spatial distribution of precipitation and topography must evolve together. Large gradients in  
35 precipitation (factors of 2- 4) over short distances (~10-40km) are tied to topography and persist  
36 over years to decades of measurement in the European Alps (Frei and Schär, 1996), the Himalaya  
37 (Anders et al., 2006; Barros et al., 2006) and the Olympic Mountains of Washington State (Anders  
38 et al., 2007). Spatial patterning of precipitation linked to topography has clear potential to influence  
39 landscape evolution.

40

41 A coupled model combining the linear orographic precipitation model (Smith and Barstad, 2004)  
42 and the CASCADE landscape evolution model (Braun and Sambridge, 1997) was developed to  
43 explore the co-evolution of precipitation and topography. The landscape evolution model  
44 represents fluvial erosion via the unit stream power model of fluvial incision (exponent of  $\frac{1}{2}$  on  
45 discharge, 1 on slope) It also includes a threshold slope set at 30 degrees to represent hillslope  
46 processes. The model is run at a spatial resolution of 1km, thus, fluvial processes dominate

47 landscape evolution. A simple fluvial incision model isolates the effects of spatially variable  
48 precipitation without additional factors such as variability in discharge or sediment in the river  
49 channel, which are neglected here although they are likely important in real systems for some time  
50 and length scales. A limited set of simulations confirm that for other common fluvial incision laws  
51 (shear stress and total stream power) results remain similar.

52

53 The linear orographic precipitation model provides an idealized representation of the relationship  
54 between precipitation and topography. The air is assumed saturated through the troposphere and  
55 has an adiabatic temperature profile. Horizontal wind speed and direction are constant in space and  
56 time. Wind speed and direction, surface temperature, and the moist static stability of the  
57 atmosphere (resistance to flow over topography) are imposed (Smith and Barstad, 2004). The flow  
58 of air over topography is then computed to determine where and how rapidly air is rising. In  
59 regions of rising air, adiabatic cooling leads to supersaturation and condensation of water vapor. A  
60 delay time represents the characteristic time scale over which water vapor is converted into  
61 precipitation hitting the ground. The delay time includes the characteristic time from the initial  
62 condensation of cloud droplets to the growth of rain drops or snow flakes large enough to have a  
63 downward directed velocity. In the atmosphere, initial nucleation of water vapor into cloud  
64 droplets of ~10 microns in diameter is followed by growth of about two orders of magnitude to  
65 reach the size of typical falling particles (e.g., Rogers and Yau, 1989). Once droplets are large  
66 enough to fall, they are still advected by the horizontal winds. The time taken for the precipitation  
67 to reach the ground depends on both the terminal velocity and the elevation at which the  
68 precipitation forms and is also included in the delay time. Different choices of delay time can  
69 simulate observed patterns of precipitation in different settings (e.g. Barstad and Smith, 2005).

70

71

72 The steady-state reached in this coupled system of precipitation and landscape evolution is  
73 dependent on two non-dimensional factors that together are the dominant controls on the  
74 precipitation pattern (Barstad and Smith, 2005). These two factors depend on external climatic  
75 conditions and also on the width of the mountain range. The first factor is the non-dimensional  
76 moisture scale height, defined as

$$\tilde{H} = \frac{N_m H_w}{U} \quad (1)$$

78

79 where  $N_m$  is the moist Brunt-Väisälä frequency, a measure of the resistance of the air to flow over  
80 topography,  $H_w$  is the moist layer depth, which depends on the surface temperature, and  $U$  is the  
81 wind speed. The lengths considered are the moisture scale height and the depth of penetration of  
82 the lifting generated by topography. More moisture is available if waves propagate through the  
83 entire moist layer depth than if waves do not lift the entire moist part of the atmosphere. Thus, this  
84 factor controls mainly the amount of precipitation generated. The second factor, non-dimensional  
85 delay time, is defined as

86

$$\tilde{\tau} = \frac{U\tau}{a} \quad (2)$$

88

89 where  $U$  is the wind speed,  $t$  is the delay time and  $a$  is the mountain half width. This factor  
90 compares the distance precipitation is advected downstream to the size of the mountain range. It  
91 dominantly controls the precipitation pattern. As non-dimensional delay time increases,  
92 precipitation is advected farther into the center of the mountain range and, eventually, for non-  
93 dimensional delay time greater than 1, to the lee of the range.

94  
95 Anders (2005) explored the entire plausible parameter space of the coupled model in terms of these  
96 two non-dimensional parameters and concluded that both the amount of precipitation and the  
97 spatial distribution of precipitation are crucial in determining the characteristics of topography.  
98 The relationship between precipitation amounts and the form of steady-state topography has been  
99 studied previously (e.g., Bonnet and Crave, 2003; Whipple and Meade, 2006). When the uplift  
100 rate is held constant, and precipitation is increased uniformly the erosion rate required to balance  
101 uplift can be achieved with lower slopes, therefore lower slopes and lower relief are found at  
102 steady-state when compared to drier climates. The importance of the spatial distribution of  
103 precipitation in a coupled system has not been previously examined, to our knowledge, except in  
104 the case of a rain-shadow at the scale of the entire mountain range (e.g. Koons, 1989; Willett,  
105 1999). In this paper we examine the impact of changes in the spatial pattern of precipitation on the  
106 evolving coupled system.

107

## 108 **Model Results**

109

110 To investigate the impact of changing precipitation patterns on steady-state topography the non-  
111 dimensional delay time was varied across a large range of reasonable values with non-dimensional

112 moisture scale height held constant at an intermediate value (1.6). Model parameters fixed for all  
113 runs include the domain size (64 by 256 grid points), time step (1 year), uplift rate(2mm/yr), fluvial  
114 incision constant ( $6 \times 10^{-6} \text{ m}^{-1/2}\text{yr}^{-1/2}$ ) wind speed (10 m/s), surface temperature (280 K), moist  
115 Brunt-Väisälä frequency, (0.007/s), and the fraction of time that precipitation occurs (0.034).  
116 Delay time was varied from 200s to 2000s to produce changes in the non-dimensional delay time  
117 from 0.1 to 1.3. In addition to controlling the precipitation pattern, changes in the delay time also  
118 produce moderate changes in precipitation amounts which impact the resultant topography by  
119 adding a tendency for lower slopes with increased precipitation, as found in previous studies.  
120 However, the precipitation patterns produce additional dramatic changes in morphology, discussed  
121 below, that cannot be accounted for with uniform changes in precipitation amounts.

122  
123 All simulations were run until a complete steady-state was reached. To facilitate comparison of  
124 topographies, one set of model runs was designed to maintain a constant mountain half-width. In  
125 these runs, winds come from ten equally spaced directions centered to be perpendicular to the long  
126 side of the model domain. The 10 resulting precipitation patterns are equally weighted to produce  
127 a composite precipitation pattern. These simulations result in ranges without rain shadows, but still  
128 create spatial variability in precipitation that is tied to topography. Changes in the non-dimensional  
129 delay time produce significant changes in both precipitation patterns and topography. Two spatial  
130 scales are examined in greater detail: that of the entire mountain range (~60 km) and that of  
131 individual drainage basins (~10 km).

132  
133 At the largest scale, the non-dimensional delay time has a profound impact on topography and  
134 precipitation patterns (Figure 1). For small non-dimensional delay times, maximum precipitation is

135 centered on the flanks of the mountain range and the center is relatively dry. Precipitation is highly  
136 variable across the domain. The resulting topography reaches high mean and maximum elevation,  
137 rises steeply toward center of the range, and has broad plains at lower elevations. In contrast, when  
138 the non-dimensional delay time is long, precipitation reaches a maximum in the center of the range  
139 and is less variable across the range. Despite a decrease in mean precipitation, the mean and  
140 maximum elevation are lower than in a case of short non-dimensional delay time. The slope of the  
141 mean topography is lower and more uniform than in the case of short delay time.

142  
143 These topographic changes highlight the importance of the distribution of precipitation along river  
144 channels in shaping landscapes. At long delay times, precipitation increases toward the drainage  
145 divide in trunk streams, which allows river slopes to increase more slowly than if precipitation  
146 were uniform. At short delay times, precipitation decreases toward the divide in trunk streams  
147 forcing them to steepen more quickly than in the case of uniform precipitation. This is consistent  
148 with the behavior of modeled one-dimensional river channels under variable precipitation (Roe et  
149 al., 2002). In the model, such changes in the concavity of streams are propagated throughout the  
150 landscape. The amount of precipitation delivered to the center of the range controls mean and  
151 maximum elevation, such that for long non-dimensional delay times it is possible for the steady-  
152 state range to be lower than in a case with short delay times despite lower precipitation on average  
153 in the long-delay time case.

154  
155 In addition to the cases described above which have no prevailing wind direction, cases with a  
156 strong prevailing wind direction perpendicular to the strike of the range were examined (Figure 2).  
157 At the range scale, a preferred wind direction produces a rain shadow and an asymmetric

158 topography. The main drainage divide is displaced downwind and the highest peaks are located  
159 even farther downwind than the divide (Figure 2). These features all vary with non-dimensional  
160 delay time. For short non-dimensional delay time the precipitation rate is very high on the lower  
161 windward flank of the range and mean and maximum elevation in the range interior are high. As  
162 delay time increases, precipitation on the lee side increases and precipitation on the windward side  
163 decreases, making the rain shadow less pronounced. The degree of displacement of the drainage  
164 divide reaches a maximum at moderate non-dimensional delay time as there is sufficient  
165 precipitation in the headwaters of windward-side rivers to allow them to capture lee-side area and a  
166 large enough difference between windward and leeward side precipitation so that the lee-side rivers  
167 cannot compete.

168

## 169 **Interpretation of Results and Implications**

170

171 The coupled model of orographic precipitation and landscape evolution demonstrates that the  
172 feedback between precipitation and topography is a major control on the modeled steady-state  
173 topography at the scale of the entire range and at the scale of individual ridges and valleys. Spatial  
174 patterning of precipitation is a first-order factor in determining the morphology of these modeled  
175 landscapes. The spatial patterns of precipitation produced are reasonable when compared to long  
176 term precipitation patterns measured in mountain ranges (e.g., Smith et al., 2005, Smith and Evans,  
177 2007; Anders et al., 2007). Thus, the model demonstrates the potential for observed spatial  
178 variability in precipitation to have a large impact on topography when the two equilibrate with one  
179 another. Spatial variability in precipitation is a primary feature of mountain climates and in has  
180 been shown to be persistent over timescales from years to decades in several ranges (e.g., Frei and

181 Schär, 1996; Anders et al., 2006; 2007) Is it reasonable to expect a geomorphic signature of the  
182 feedback between precipitation and topography may be present in real topography?

183

184 We recognize that the idealized coupled model and the assumptions implicit in it make direct  
185 interpretation of the results in terms of natural systems difficult. The parameters in the  
186 precipitation model should not be interpreted too rigidly when considering natural climatic  
187 systems. The spatial pattern of precipitation in the coupled model is controlled by the non-  
188 dimensional delay time which compares the characteristic distance precipitation is advected with  
189 the width of the mountain range (equation 2). If range width increases while the advection distance  
190 of precipitation remains the same, precipitation tends to fall out before reaching the center of the  
191 range. Precipitation decreases in the center of the range, maximum elevations increase, and river  
192 profiles steepen relative to a narrower orogen. The model suggests that as a range grows in width  
193 in a stable climatic setting, the efficiency of the climate at eroding the high topography decreases  
194 because less precipitation penetrates into the core of the range. This implication is consistent with  
195 the observation that the width of the Andes increases in the vicinity of the high and dry Altiplano  
196 (Montgomery et al., 2001).

197

198 The characteristic distance precipitation is advected is more difficult to interpret than range width.  
199 In the model, a characteristic wind speed and the delay time determine this distance. These  
200 quantities are difficult to measure and how they may vary between ranges or over long timescales  
201 is unknown Regional storm climatology is difficult for global climate models (CGMs) to  
202 reproduce. The position and intensity of storm tracks during the last glacial maximum as modeled  
203 by a set of GCMs varies considerably from one model to another, even in the sign of changes

204 (Kageyama et al., 1999). Thus, understanding how storm wind speed may vary in space and time  
205 is difficult. Likewise, the delay time represents numerous microphysical processes that are difficult  
206 to observe directly and are virtually impossible to constrain over long timescales. However, one  
207 component of the advection distance is well characterized, namely, the strong control of  
208 precipitation phase on terminal velocity of falling precipitation. Rain droplets fall at 5-10 m/s,  
209 while snow falls an order of magnitude more slowly at 0.5-1 m/s (e.g., Locatell and Hobbs, 1974;  
210 Braziersmith, 1992). The much slower fall speed of snow allows it to be advected further  
211 downstream than rain. In the midlatitudes, it is common for rain at the ground's surface to have  
212 begun as frozen precipitation. In cool climates relative to warm climates, a larger fraction of  
213 precipitation will fall as snow for a longer portion of its descent increasing the distance that  
214 precipitation is advected.

215  
216 The association of decreasing mean temperature with increasing advection distance is consistent  
217 with the few comparisons of the linear orographic precipitation model to observations. The work  
218 available suggests a systematic relationship between the delay time and the mean annual  
219 temperature (Figure 3). Case studies of individual storm events in the Wasatch Range of Utah, the  
220 southern California Coast Range and in the European Alps have produced estimates of delay time  
221 (Barstad and Smith, 2005). The long-term climatological pattern of precipitation and isotopic  
222 depletion of precipitation have been used to constrain delay times for the Oregon Coast Ranges and  
223 Cascades (Smith et al., 2005), the southern Andes (Smith and Evans, 2007), and the Olympics  
224 Mountains of Washington State (Anders et al., 2007). Considered together, these studies suggest  
225 that cooler climates produce precipitation patterns consistent with longer delay times and longer  
226 advection distances than warmer climates (Figure 3).

227

228 There are caveats in the association between temperature and delay time, and especially in the  
229 prediction of advection distances, as the mechanisms behind the observed relationship are not well  
230 understood. In particular, cool and warm climates not only differ in the fraction of precipitation  
231 that falls as snow, but also in the characteristic height at which precipitation forms. In cool  
232 climates atmospheric moisture is limited to a shallower layer so precipitation has a shorter distance  
233 to fall. This will tend to decrease the delay time, partially counteracting the slower fall speed of  
234 snow, relative to rain. The moist layer depth changes by a factor of 2-3 from cool to warm  
235 climates, which is small compared to the order of magnitude difference in the fall speed of rain vs.  
236 snow, suggesting that the dominant effect is the slower fall speed of snow in a cool climate.

237 Microphysical processes of growth are dependent on the temperature and phase of the droplets.

238 The processes contributing to growth are difficult to constrain and are neglected in this orographic  
239 precipitation model. In particular, it is difficult to predict if a cool climate will differ significantly  
240 from a warm climate in terms of the average time for growth of precipitation particles from cloud  
241 water. In summary, more research is necessary to better understand the relationship of advection  
242 distance and climate. Current knowledge allows us to say that there is variability in the  
243 characteristic delay time from range to range and this variability is consistent with increasing delay  
244 time in regions with decreasing mean annual temperature (Figure 3). This indicates a shift toward  
245 more uniform precipitation in cooler mountain ranges with lower maximum topography and lower  
246 channel concavities relative to warmer mountain ranges. In a cooler climate the tendency for more  
247 precipitation to fall in the center of the range will to increase erosional efficiency. Although our  
248 results do not include effects of a difference between fluvial and glacial erosion, they are consistent  
249 with an increase in erosion rates during climatic cooling.

250

251 A self-consistent coupled model of orographic precipitation and landscape evolution demonstrates  
252 that feedbacks between small-scale precipitation patterns and topography have the potential to be a  
253 first order control on mountain geomorphology. In the idealized model, a range of behavior from  
254 nearly uniform spatial distributions of precipitation to precipitation patterns that are closely coupled  
255 to topographic features <10 km in scale are possible. Maximum elevation, channel concavity, and  
256 ridge-valley relief of the steady-state topography are correlated with the non-dimensional delay  
257 time. The model results can be interpreted as reflect effects of variations in climate with cooler  
258 climates associated with larger non-dimensional delay times, a tendency for more spatially uniform  
259 precipitation, lower maximum elevations and lower channel concavities relative to warmer  
260 climates. Not only is the spatial patterning of precipitation sufficient to produce large changes in  
261 topography, but the nature of the precipitation patterns is also likely to vary as a function of  
262 climate. Therefore, we expect the feedback between precipitation patterns and topography to be  
263 manifested in different ways in different climatic settings. This link between atmospheric and  
264 geomorphic processes emphasizes the coupled nature of the earth system and represents an under-  
265 explored area in the relationships between climate, tectonics and erosion.

266

### 267 **Acknowledgements**

268 Thanks to Jean Braun, Ronald Smith, and Idar Barstad for sharing their model codes. Thanks to  
269 Drew Stolar for advice on model set-up.

270

### 271 **References**

272

273 Anders, A.M., 2005, The co-evolution of precipitation and topography [Ph.D. Thesis]: Seattle,  
274 University of Washington, 249 p.

275  
276 Anders, A.M., Roe, G.H., Hallet, B., Montgomery, D.R., Finnegan, N.J., and Putkonen, J., 2006,  
277 Spatial patterns of precipitation and topography in the Himalaya in Willett, S.D., Hovius, N.,  
278 Brandon, M.T., and Fisher D., eds., Tectonics, Climate and Landscape Evolution: Geological  
279 Society of America Special Paper 398, p. 39-53.

280  
281 Anders, A.M, Roe, G.H., Durran, D.R., and Minder, J.R.,2007 Small-scale spatial gradients in  
282 climatological precipitation on the Olympic Peninsula, Journal of Hydrometeorology, (in press).

283  
284 Barros, A.P., Chiao, S., Lang, T.J., Burbank, D., and Putkonen, J., 2006, From weather to climate –  
285 Seasonal and interannual variability of storms and implications for erosion processes in the  
286 Himalaya, in Willett, S.D., Hovius, N., Brandon, M.T., and Fisher D., eds., Tectonics, Climate and  
287 Landscape Evolution: Geological Society of America Special Paper 398, p. 17-38.

288 Barstad, I., and Smith, R.B. 2005, Evaluation of an orographic precipitation model: Journal of  
289 Hydrometeorology, v. 6, p. 85-99.

290  
291 Bonnet, S. and Crave, A., 2003, Landscape response to climate change: Insights from experimental  
292 modeling and implications for tectonic versus climatic uplift of topography: Geology, v. 31, p. 123-  
293 126.

294

295 Braziersmith, P.R., 1992, On the shape and fall velocities of raindrops: Quarterly Journal of the  
296 Royal Meteorological Society, v. 118, p. 749-766.  
297

298 Braun, J., and Sambridge, M., 1997, Modelling landscape evolution on geological time scales: a  
299 new method based on irregular spatial discretization: Basin Research, v. 9, p. 27-52.  
300  
301

302 Frei, C., and Schär, C., 1998, A precipitation climatology of the Alps from high-resolution rain-  
303 gauge observations: International Journal of Climatology, v. 18, p. 873-900.  
304  
305

306 Hallet, B., 1996, Glacial quarrying: a simple theoretical model, Annals of Glaciology, v. 22, p.1-8.  
307

308 Kageyama, M., Valdes, P.J., Ramstein, G., Hewitt, C. and Wyputta, U., 1999, Northern hemisphere  
309 storm tracks in present day and last glacial maximum climate simulations: a comparison of  
310 European PMIP models: Journal of Climate, v. 12, p. 742-760.  
311

312 Koons, P.O., 1989, The topographic evolution of collisional mountain belts; a numerical look at the  
313 Southern Alps, New Zealand: Science, v. 289, p. 1041-1069.  
314

315 Locatell, J.D., and Hobbs, P.V., Fall speeds and masses of solid precipitation particles: Journal of  
316 Geophysical Research, v. 79, p. 2185-2197.  
317

318 Montgomery, D.R., Balco, G., and Willett, S.D., 2001, Climate, tectonics and the morphology of  
319 the Andes: *Geology*, v. 29, P. 579-582.  
320

321 Roe, G.H., Montgomery, D.R., and Hallet, B., 2002, Effects of orographic precipitation variations  
322 on the concavity of steady-state river profiles: *Geology*, v. 30, p. 143-146.  
323

324 Rogers, R.R. and Yau, M.K., 1989, *A short course in cloud physics*, 3rd edition: London,  
325 Butterworth-Heinemann, 308 p.  
326

327 Smith R.B. and Evans J.P., 2007, Orographic precipitation and water vapor fractionation over the  
328 southern Andes: *Journal of Hydrometeorology*, (in press).  
329

330 Smith, R.B. and Barstad, I., 2004. A linear theory of orographic precipitation: *Journal of the*  
331 *Atmospheric Sciences*, v. 61, p. 1377-1391.  
332

333 Smith, R.B., Barstad, I. and Bonneau, L. 2005, Orographic precipitation and Oregon's climate  
334 transition: *Journal of the Atmospheric Sciences*, v. 62, p. 177-191.  
335

336 Whipple, K.X., 2004, Bedrock rivers and the geomorphology of active orogens: *Annual Reviews of*  
337 *Earth and Planetary Science*, v. 32, p. 151-185.  
338

339 Whipple, K.X., and Meade, B.J., 2006, Orogen response to changes in climatic and tectonic  
340 forcing: *Earth and Planetary Science Letters*, v. 243, p. 218-228.

341

342 Willett, S.D., 1999, Orography and orography: The effects of erosion on mountain belts: Journal of  
343 Geophysical Research, v. 104, p. 28957-28981.

344

345

346 **Figure Captions**

347

348 Figure 1:

349 Panel A shows the map views of elevation and precipitation rate for steady-state ranges with short  
350 (0.1) and long (1.3) non-dimensional delay times. Winds come from ten equally spaced directions  
351 with equal frequency in these simulations. Elevation is contoured at 500 m intervals and  
352 precipitation rate at 1 m/yr intervals. Panel B shows the mean elevation and precipitation as a  
353 function of distance across the domain. Panel C is the distribution of ridge-valley relief across the  
354 range.

355

356 Figure 2:

357 Panels as in Figure 1. Results are from simulations with a preferred wind direction from the bottom  
358 in panel A and from the left in panels B and C.

359

360 Figure 3:

361 The estimated delay time is compared with mean annual temperature. Studies of individual events  
362 are shown as open diamond symbols and studies of long-term precipitation patterns are shown as  
363 filled squares.

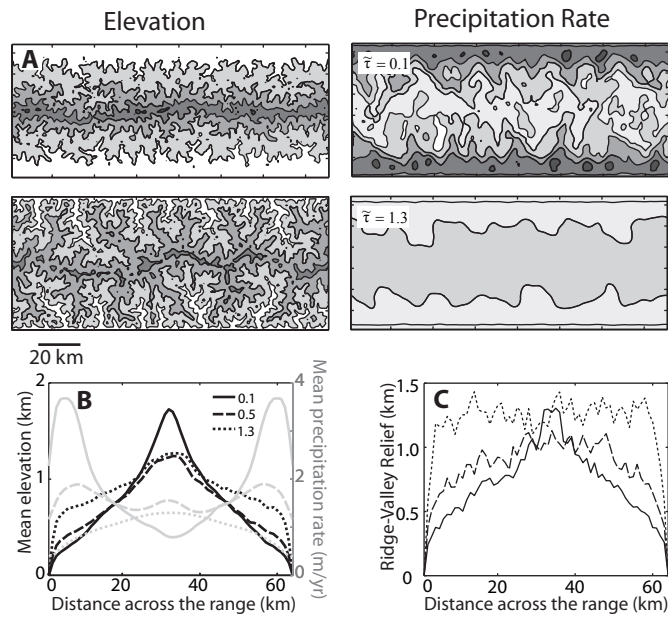


Figure 1:

Panel A shows the map views of elevation and precipitation rate for steady-state ranges with short (0.1) and long (1.3) non-dimensional delay times. Winds come from ten equally spaced directions with equal frequency in these simulations. Elevation is contoured at 500 m intervals and precipitation rate at 1 m/yr intervals. Panel B shows the mean elevation and precipitation as a function of distance across the domain. Panel C is the distribution of ridge-valley relief across the range.

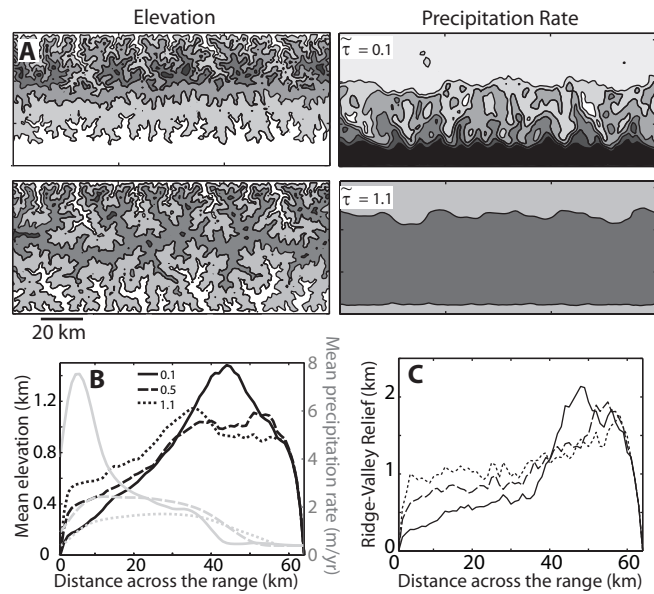


Figure 2:  
 Panels as in Figure 1. Results are from simulations with a preferred wind direction from the bottom in panel A and from the left in panels B and C.

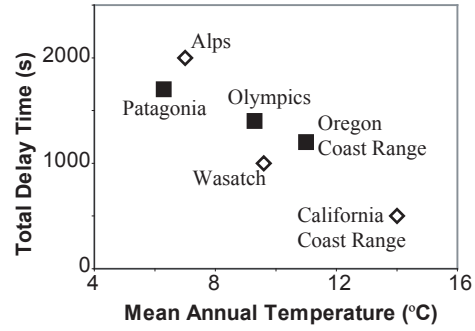


Figure 3:  
The estimated total delay time is compared with mean annual temperature. Studies of individual events are shown as open diamond symbols and studies of long-term precipitation patterns are shown as filled squares.